

Concentration and pH dependence of skeletal muscle chloride channel ClC-1

G. Y. Rychkov *†, M. Pusch ‡, D. St J. Astill *†, M. L. Roberts †, T. J. Jentsch ‡
and A. H. Bretag *†§

*Centre for Advanced Biomedical Studies, University of South Australia, North Terrace, Adelaide, South Australia 5000, Australia, †Department of Physiology, The University of Adelaide, South Australia 5005, Australia and ‡Centre for Molecular Neurobiology (ZMNH), Hamburg University, D-20246 Hamburg, Germany

1. The influence of Cl⁻ concentration and pH on gating of the skeletal muscle Cl⁻ channel, ClC-1, has been assessed using the voltage-clamp technique and the Sf-9 insect cell and *Xenopus* oocyte expression systems.
2. Hyperpolarization induces deactivating inward currents comprising a steady-state component and two exponentially decaying components, of which the faster is weakly voltage dependent and the slower strongly voltage dependent.
3. Open probability (P_o) and kinetics depend on external but not internal Cl⁻ concentration.
4. A point mutation, K585E, in human ClC-1, equivalent to a previously described mutation in the *Torpedo* electroplaque chloride channel, ClC-0, alters the $I-V$ relationship and kinetics, but retains external Cl⁻ dependence.
5. When external pH is reduced, the deactivating inward currents of ClC-1 are diminished without change in time constants while the steady-state component is enhanced.
6. In contrast, reduced internal pH slows deactivating current kinetics as its most immediately obvious action and the P_o curve is shifted in the hyperpolarizing direction. Addition of internal benzoate at low internal pH counteracts both these effects.
7. A current activated by hyperpolarization can be revealed at an external pH of 5.5 in ClC-1, which in some ways resembles currents due to the slow gates of ClC-0.
8. Gating appears to be controlled by a Cl⁻-binding site accessible only from the exterior and, possibly, by modification of this site by external protonation. Intracellular hydroxyl ions strongly affect gating either allosterically or by direct binding and blocking of the pore, an action mimicked by intracellular benzoate.

Mammalian skeletal muscle cells have a high Cl⁻ conductance, typically about 80% of total membrane conductance (Bretag, 1987). Evidence attributing the major component of macroscopic Cl⁻ conductance to the membrane protein ClC-1 has been obtained by demonstration of mutations in the *clc-1* gene in mouse (Steinmeyer *et al.* 1991*a*; Gronemeier, Condie, Prosser, Steinmeyer, Jentsch & Jockusch, 1994) and in human myotonic muscle diseases (Koch *et al.* 1992; George, Crackower, Abdalla, Hudson & Ebers, 1993) where Cl⁻ conductance is deficient, and by characterization of ClC-1 expressed in *Xenopus* oocytes (Steinmeyer, Ortland & Jentsch, 1991*b*), HEK293 cells (Pusch, Steinmeyer & Jentsch, 1994; Fahlke, Rüdél, Mitrovic, Zhou & George, 1995) and

Sf-9 insect cells (Astill, Rychkov, Clarke, Hughes, Roberts & Bretag, 1996) which show Cl⁻ currents that deactivate at hyperpolarizing potentials and saturate at depolarizing potentials, in agreement with macroscopic currents seen in muscle cells themselves (Warner, 1972; Fahlke & Rüdél, 1995). Furthermore, in a number of the human ClC-1 mutants that have been associated with myotonia, the abnormalities of Cl⁻ conductance observed in the expressed ClC-1 are sufficient to explain the myotonic symptoms (Steinmeyer, Lorenz, Pusch, Koch & Jentsch, 1994; Fahlke *et al.* 1995; Pusch, Steinmeyer, Koch & Jentsch, 1995*b*). Obviously, normal excitability of muscle cells relies on the presence and proper function of ClC-1 channels.

§ To whom correspondence should be addressed at the Centre for Advanced Biomedical Studies.

Owing to its apparently small unitary conductance (Pusch *et al.* 1994), CIC-1 has not been amenable to the extensive single channel analysis undertaken with its *Torpedo* electroplaque analogue, CIC-0 (Miller, 1982; Richard & Miller, 1990; Bauer, Steinmeyer, Schwarz & Jentsch, 1991; Middleton, Pheasant & Miller, 1994). However, ensemble behaviour of members of the CIC family of channels can easily be compared in the heterologous expression systems. Among the most interesting characteristics of CIC-0 is its peculiar double-barrelled gating with a fast, depolarization-activated, hyperpolarization-deactivated gate operating on each proto-channel and a slow gate with opposite voltage dependence operating on both protochannels simultaneously (Miller, 1982). In contrast, studies with CIC-1 have suggested that its gating is solely of the fast variety (Steinmeyer *et al.* 1991*b*), while for CIC-2, slow gating which looks similar to that seen in CIC-0 is predominant (Thiemann, Gründer, Pusch & Jentsch, 1992; Gründer, Thiemann, Pusch & Jentsch, 1992). In CIC-0, behaviour of the fast gate depends on the nature and concentration of the external permeant anion, channel opening being favoured by external Cl⁻ (Pusch, Ludewig, Rehfeldt & Jentsch, 1995*a*). Microscopically, this is seen as an asymmetry in transitions between closed and open states (Richard & Miller, 1990) and implies that the conformation of the channel is coupled to an anion binding site exposed to the external anionic environment (Pusch *et al.* 1995*a*). It has thus been concluded that the voltage-dependent gating observed in CIC-0 is conferred by the permeating ion itself, which acts as the gating charge (Pusch *et al.* 1995*a*). With respect to CIC-1, this explanation has been challenged by Fahlke *et al.* (1995) and Fahlke, Rosenbohm, Mitrovic, George & Rüdell (1996), who extend the prevailing view of voltage-dependent gating, implicating voltage sensors in the channel structure. Our analysis of CIC-1 argues against the Fahlke model and provides strong new evidence for the more radical proposal of Pusch *et al.* (1995*a*).

It has long been known that the Cl⁻ conductance of muscle cells is greatly reduced by low pH (Hutter & Warner, 1967; Palade & Barchi, 1977) and the usual hyperpolarization-deactivated currents are replaced by hyperpolarization-activated currents (Warner, 1972). We find, in addition, that CIC-1 gating is differentially sensitive to external and internal pH and that slow gating behaviour can be induced in CIC-1 when pH is appropriately manipulated.

METHODS

Rat CIC-1 (rCIC-1) was expressed in Sf-9 insect cells as described in detail previously (Astill *et al.* 1996). Cultured Sf-9 cells were infected, at a multiplicity of infection of 50, with baculovirus clones BVDA6.3 and BVDA2.1 containing rCIC-1 cDNA inserted in forward and reverse orientations, respectively, the latter (BVDA2.1 infected) acting as negative controls of expression. Cells were grown in Grace's insect cell culture medium (Gibco) supplemented with 0.333% w/v lactalbumin hydrolysate, 0.333% w/v yeastolate (Difco, Detroit, MI, USA) and 10% v/v bovine fetal serum (CSL, Melbourne, Australia). Incubations were at 28–30 °C in air. Cells

were maintained in monolayer cultures and were passaged at ca 80% confluence (twice weekly). Cells to be infected were seeded at low density in 35 mm Petri dishes and incubated until ca 50% confluence (24–48 h) before inoculation and further incubation for 24–30 h. Following incubation, infected cells were seeded onto glass coverslips and maintained at room temperature in cell culture medium until required. Before patch-clamping, cells were rinsed in bath solution to remove excess culture medium. Patch-clamp experiments were performed between 28 and 34 h postinfection, at which time expression of the rCIC-1 protein has been clearly demonstrated (Astill *et al.* 1996).

General electrophysiological methods were as described by Astill *et al.* (1996). Cell-attached, whole-cell patch-clamping was performed directly on Sf-9 cells using a List EPC7 patch-clamp amplifier and associated standard patch-clamping equipment. The usual bath solution contained (mM): NaCl, 170; MgSO₄, 2; CaCl₂, 2; and Hepes, 10; adjusted to pH 7.5 with NaOH. Lower Cl⁻ concentrations were achieved by equimolar substitution of sodium glutamate or glucose for NaCl and, if necessary, calcium gluconate for CaCl₂. Electrodes were borosilicate glass, pulled on a Kopf two-step puller, and had a resistance of 2–4 MΩ. Electrodes were filled with a normal internal solution containing (mM): KCl, 40; potassium glutamate, 120; EGTA-Na, 10; and Hepes, 10; adjusted to pH 7.2 with NaOH. Internal Cl⁻ concentrations were adjusted by modifying the KCl to potassium glutamate proportions. Bath and electrode solutions of higher and lower pH were prepared using Tris, Hepes or Mes buffers (10 mM) and titrating with glutamic acid or NaOH as appropriate. When necessary, pentobarbitone (0.5 mM) was used to block native anion channels in Sf-9 cells (Birner, Tierney, Howitt, Cox & Gage, 1992). Data were collected, filtered at 3 kHz and analysed on an IBM-compatible PC using pCLAMP v5.5 software (Axon Instruments). Potentials listed are pipette potentials expressed as intracellular potentials relative to outside zero. Liquid junction potentials between the bath and electrode solutions were estimated by using JPCalc (Barry, 1994) and corrected where specified. Experiments were conducted at room temperatures of 24 ± 1 °C.

Wild-type human CIC-1 (WT hCIC-1) and the mutant K585E were expressed in *Xenopus* oocytes. Construction of the mutant, RNA synthesis, oocyte injection, and two-electrode voltage-clamping of oocytes were performed as described by Pusch *et al.* (1995*a*). For oocyte experiments, the standard bath solution was ND96 (Steinmeyer *et al.* 1991*b*), which contained (mM): NaCl, 96; KCl, 2; CaCl₂, 1.8; MgCl₂, 1; Hepes, 5; adjusted to pH 7.4 with NaOH. In some experiments 80 mM NaCl was replaced on an equimolar basis by sodium glutamate (leaving 23.6 mM Cl⁻).

Many of the results have been fitted by Boltzmann distributions of the form:

$$X(V) = X_o + (1 - X_o)/(1 + \exp((V_{1/2} - V)/k)),$$

where X_o is an offset, V is the transmembrane potential, $V_{1/2}$ is the potential at which $X = (1 + X_o)/2$, and k is the slope factor.

RESULTS

Kinetics and open probability of rCIC-1 depend on external Cl⁻ concentration

In our whole-cell patch-clamp studies of Sf-9 cells expressing rCIC-1, inwardly rectifying macroscopic Cl⁻ currents rapidly deactivated at hyperpolarizing potentials (Fig. 1). Since the rate of deactivation became slower during the initial

Table 1. Effects of pH_i, external Cl⁻ concentration and the mutation K585E on time constants (ms) of the fast (τ₁) and slow (τ₂) exponential components of deactivating currents

	n	[Cl ⁻] _o (mM)	pH _o	pH _i	-160 mV*	-140 mV*	-120 mV*	-100 mV*	-80 mV*	-60 mV*	-40 mV*	-20 mV*	0 mV*	20 mV*
rClC-1														
τ ₁	23	174	7.5	7.2	—	7.1 ± 0.7	5.9 ± 0.7	5.1 ± 0.6	4.0 ± 0.7	3.3 ± 0.9	—	—	—	—
τ ₂	23	174	7.5	7.2	—	22.0 ± 3.0	26.1 ± 6.5	40.0 ± 9.4	58.4 ± 9.5	78.4 ± 16.5	—	—	—	—
τ ₁	9	40	7.5	7.2	—	4.6 ± 1.2	4.7 ± 0.6	5.1 ± 0.9	4.6 ± 0.9	4.1 ± 0.8	3.3 ± 0.6	—	—	—
τ ₂	9	40	7.5	7.2	—	14.5 ± 2.0	16.1 ± 3.4	18.2 ± 3.0	24.6 ± 5.3	39.9 ± 5.6	56.7 ± 12.0	—	—	—
τ ₁	8	8	7.5	7.2	—	—	3.9 ± 0.2	4.5 ± 0.4	5.1 ± 0.6	5.1 ± 0.7	4.7 ± 0.5	4.1 ± 0.5	2.6 ± 0.8	—
τ ₂	8	8	7.5	7.2	—	—	14.5 ± 3.8	15.0 ± 1.9	18.0 ± 3.2	20.2 ± 2.8	28.3 ± 4.0	37.8 ± 12.3	48.1 ± 8.0	—
τ ₁	4	4	7.5	7.2	—	—	3.9 ± 0.6	4.6 ± 0.7	5.1 ± 0.7	4.9 ± 0.2	5.1 ± 0.4	4.1 ± 0.5	2.8 ± 0.7	2.9 ± 1.3
τ ₂	4	4	7.5	7.2	—	—	13.4 ± 3.8	15.9 ± 1.9	17.9 ± 3.7	20.0 ± 2.7	23.5 ± 3.0	32.4 ± 4.3	38.6 ± 7.5	50.0 ± 18.0
τ ₁	3	174	6.5	7.2	—	7.2 ± 0.8	7.4 ± 0.5	6.3 ± 0.4	5.1 ± 0.8	3.9 ± 0.5	—	—	—	—
τ ₂	3	174	6.5	7.2	—	18.6 ± 3.5	24.8 ± 1.8	32.4 ± 2.1	44.3 ± 9.2	61.2 ± 11.2	—	—	—	—
τ ₁	3	174	6.0	7.2	—	6.6 ± 0.7	7.1 ± 0.3	7.4 ± 1.3	6.0 ± 0.4	5.0 ± 0.4	—	—	—	—
τ ₂	3	174	6.0	7.2	—	27.6 ± 3.1	26.7 ± 4.6	40.1 ± 8.6	56.3 ± 5.1	67.2 ± 11.2	—	—	—	—
τ ₁	4	174	7.5	8.0	—	2.1 ± 0.15	2.5 ± 0.17	2.7 ± 0.22	2.5 ± 0.20	1.9 ± 0.14	1.4 ± 0.40	—	—	—
τ ₂	4	174	7.5	8.0	—	13.5 ± 2.1	14.4 ± 1.2	17.1 ± 0.9	23.0 ± 4.6	30.9 ± 6.1	34.0 ± 11.2	—	—	—
τ ₁	5	174	7.5	6.2	—	18.8 ± 2.0	16.2 ± 2.5	14.7 ± 2.3	8.7 ± 1.3	—	—	—	—	—
τ ₂	5	174	7.5	6.2	—	65.6 ± 15.6	98.8 ± 21.3	126.0 ± 26.0	158.0 ± 14.4	—	—	—	—	—
WT hClC-1														
τ ₁	10	103.6	7.4	—	2.8 ± 0.45	3.7 ± 0.7	4.7 ± 1.4	4.4 ± 0.7	6.4 ± 2.3	—	—	—	—	—
τ ₂	10	103.6	7.4	—	7.7 ± 2.6	13.1 ± 3.6	22.5 ± 9.0	31.0 ± 7.2	51.2 ± 11.5	—	—	—	—	—
τ ₁	10	23.6	7.4	—	—	2.8 ± 0.3	3.7 ± 1.1	4.9 ± 0.8	5.8 ± 1.4	7.1 ± 1.6	5.4 ± 1.3	—	—	—
τ ₂	10	23.6	7.4	—	—	9.7 ± 3.5	16.5 ± 6.0	22.0 ± 7.1	30.5 ± 9.3	47.4 ± 12.3	53.1 ± 10.2	—	—	—
K585E hClC-1														
τ ₂	4	103.6	7.4	—	34.6 ± 2.6	46.4 ± 7.6	49.3 ± 3.3	55.7 ± 2.1	56.0 ± 5.2	67.2 ± 13.4	—	—	—	—
τ ₂	4	23.6	7.4	—	25.0 ± 1.3	32.1 ± 4.8	35.1 ± 2.3	42.4 ± 2.3	48.7 ± 2.3	54.9 ± 1.6	—	—	—	—

* Nominal externally applied voltage. For strict comparison, the following correction factors must be applied to the nominal voltages listed for Sf-9 experiments (rClC-1) to account for differing liquid junction potentials at each Cl⁻ concentration: 174 mM Cl⁻, -14 mV; 40 mM Cl⁻, -6 mV; 8 mM Cl⁻, -4 mV; and 4 mM Cl⁻, -3 mV. For oocyte experiments (hClC-1), a correction factor of +8 mV must be made to the nominal voltages listed for data obtained at 23.6 mM Cl⁻. Results expressed as means ± s.d.

5–10 min after achieving whole-cell configuration (30–50% increase in the time constants), wherever comparisons were required, a sufficient time was allowed for stabilization of conditions before making kinetic analyses. With lower resistance electrodes, these kinetic changes occurred more

rapidly but were not influenced by addition of ATP or cAMP to the pipette solution.

When external Cl⁻ was reduced by substitution with apparently impermeant anions, such as glutamate, kinetic parameters of Cl⁻ current deactivation were substantially

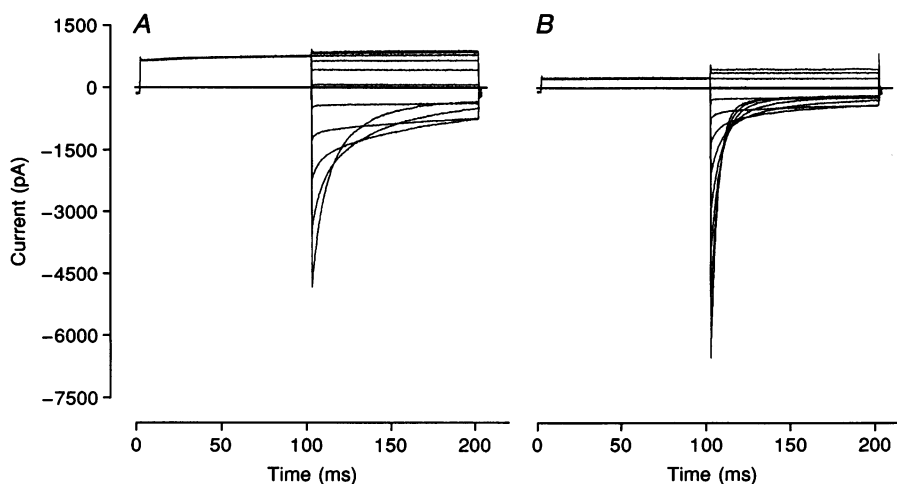


Figure 1. Voltage- and Cl⁻-dependent gating of rClC-1 expressed in Sf-9 cells

Chloride currents were recorded in response to a voltage protocol consisting of 100 ms voltage steps ranging from -120 to +80 mV (20 mV increments) after a 100 ms prepulse to +40 mV from holding potentials of -30 mV (A) and +30 mV (B) for an external [Cl⁻] of 174 mM (A) or 8 mM (B).

Table 2. Effects of pH and external Cl^- concentration on $V_{1/2}$ and slope factor (k) determined by fitting Boltzmann distributions to apparent P_o .

$[\text{Cl}^-]_o$ (mM)	n	pH _o	pH _i	$V_{1/2}$ (mV)	Slope factor
174	9	7.5	7.2	-88.2 ± 1.2	-21.3 ± 0.8
40	7	7.5	7.2	-56.0 ± 1.1	-21.1 ± 0.6
8	4	7.5	7.2	-16.0 ± 1.0	-22.0 ± 0.7
4	4	7.5	7.2	-2.5 ± 0.4	-23.0 ± 0.7
174	4	7.5	8.0	-72.0 ± 0.8	-21.1 ± 1.1
174	4	7.5	6.2	-116.1 ± 0.5	-26.3 ± 0.5
174	2	7.5	5.6	-138.4 ± 0.5	-30.1 ± 0.6
8	3	7.5	6.2	-45.3 ± 1.4	-26.9 ± 1.2
8	2	7.5	5.6	-52.8 ± 0.6	-31.3 ± 0.7
174	3	6.5	7.2	-95.8 ± 2.0	-22.7 ± 1.1
174	3	6.0	7.2	-91.1 ± 4.1	-26.1 ± 1.8

$V_{1/2}$ values have been corrected for liquid junction potentials. Results expressed as means \pm s.d.

modified (Fig. 1A and B), whereas they were insensitive to internal Cl^- concentration. Three exponential components, with time constants of the order of milliseconds (τ_1 , referred to as 'fast'), tens of milliseconds (τ_2 , referred to as 'slow') and hundreds of milliseconds (τ_3 , referred to as 'very slow'), and a steady-state component could be extracted from these currents. The very slow, minor exponential component (τ_3) was, however, not generally separated from the steady state because of the difficulty in extracting it from

relatively short duration currents. 'Steady state' therefore implies (τ_3 + steady state) unless otherwise indicated. At normal external Cl^- concentration, the components show some voltage dependence (Table 1), with the fast component tending to become faster at less hyperpolarizing potentials ($\tau_1 = 7.1 \pm 0.7$ and 3.3 ± 0.9 ms, $n = 23$, at -140 and -60 mV, respectively, with statistically significant differences ($P < 0.05$) between -140 and -80 or -60 mV). The slow component, however, becomes several times slower

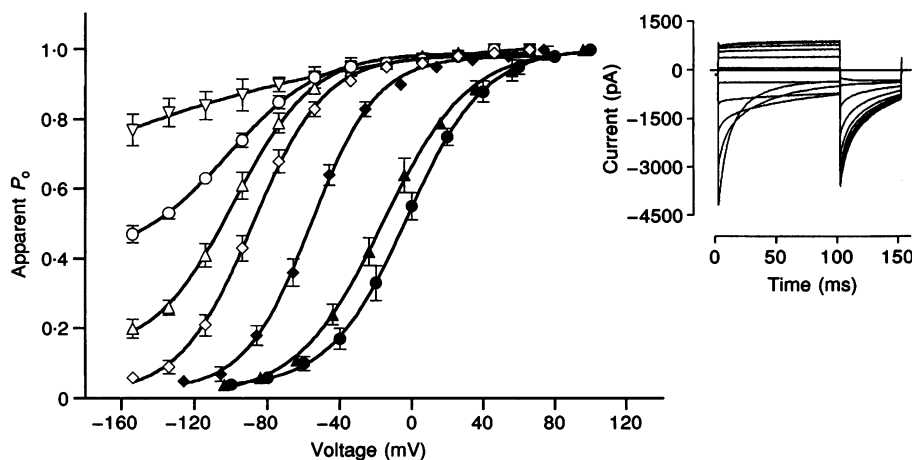


Figure 2. Apparent P_o of rClC-1 as a function of the membrane potential at different external pH values and Cl^- concentrations

Current traces in Sf-9 cells expressing rClC-1 were elicited by patch-clamp test pulses at 20 mV increments, as shown in the inset example for pulses between -120 and $+80$ mV with a constant 'tail' pulse of -100 mV. Apparent P_o was determined from the tail currents by normalizing to the maximum tail current flowing after the most positive test pulses. Internal pH was 7.2 in all experiments. The reference curve for these experiments was that obtained with an external $[\text{Cl}^-]$ of 174 mM and an external pH of 7.5 (\diamond). Results (open symbols all at external $[\text{Cl}^-]$ concentration of 174 mM, filled symbols all at pH_o of 7.5) are plotted as a means \pm s.d.: \triangle , pH 6.5; \circ , pH 6.0; ∇ , pH 5.5; \blacklozenge , 40 mM $[\text{Cl}^-]_o$; \blacktriangle , 8 mM $[\text{Cl}^-]_o$; and \bullet , 4 mM $[\text{Cl}^-]_o$. Numbers in each experimental category are as listed in Table 2. The continuous lines represent fits of a Boltzmann distribution (including a constant offset, $X_o = 0.13 \pm 0.03$ for pH_o 6.5, 0.38 ± 0.03 for pH_o 6.0 and 0.78 ± 0.07 for pH_o 5.5). Liquid junction potentials have been corrected.

over the same voltage range ($\tau_2 = 22 \pm 3.0$ and 78.4 ± 16.5 ms, $n = 23$, at -140 and -60 mV, respectively, also statistically significant, $P < 0.05$). In response to a reduction in external Cl⁻, there is a faster deactivation (Fig. 1) due almost entirely to a decrease in τ_2 which, however, retains its monotonic relationship with voltage (Table 1). Concomitantly, a weakly parabolic dependence of τ_1 on voltage appears (Table 1), although not statistically significant, with peaks in τ_1 at about -100 and -70 mV for 40 and 8 mM Cl⁻, respectively. At normal external Cl⁻ levels, the suggested weakly parabolic relationship is obscured, its peak possibly shifted too far in the hyperpolarizing direction to be discerned.

At a holding potential of -30 mV, both inward and outward currents are reduced with decreasing external Cl⁻ until the normally prominent inward currents are essentially absent at submillimolar Cl⁻ concentrations. Currents can, however, be maintained if the holding potential is adjusted to

approximate the new Cl⁻ equilibrium potential (Fig. 1B). In addition, comparison of Fig. 1A and B shows that for steps to -120 mV, as external Cl⁻ is reduced, the fast component of deactivation becomes more prominent and the slow and 'steady-state' components are less prominent. This change in relative prominence of the three components is voltage dependent and the original proportionality is restored by a depolarization of approximately 58 mV per decade of reduction in external Cl⁻ concentration.

Assuming that the deactivating currents are due to classical gating processes, peak tail currents can be used to estimate apparent open probabilities (P_o) at the steady state for each voltage (Fig. 2). As external Cl⁻ concentrations are reduced, these P_o (deactivation) curves are shifted to more depolarizing potentials (see also $V_{1/2}$ values in Table 2) in the same manner as the relative prominence of current components (described above). In all of these experiments, reduction of external Cl⁻ concentration was achieved by replacing it with

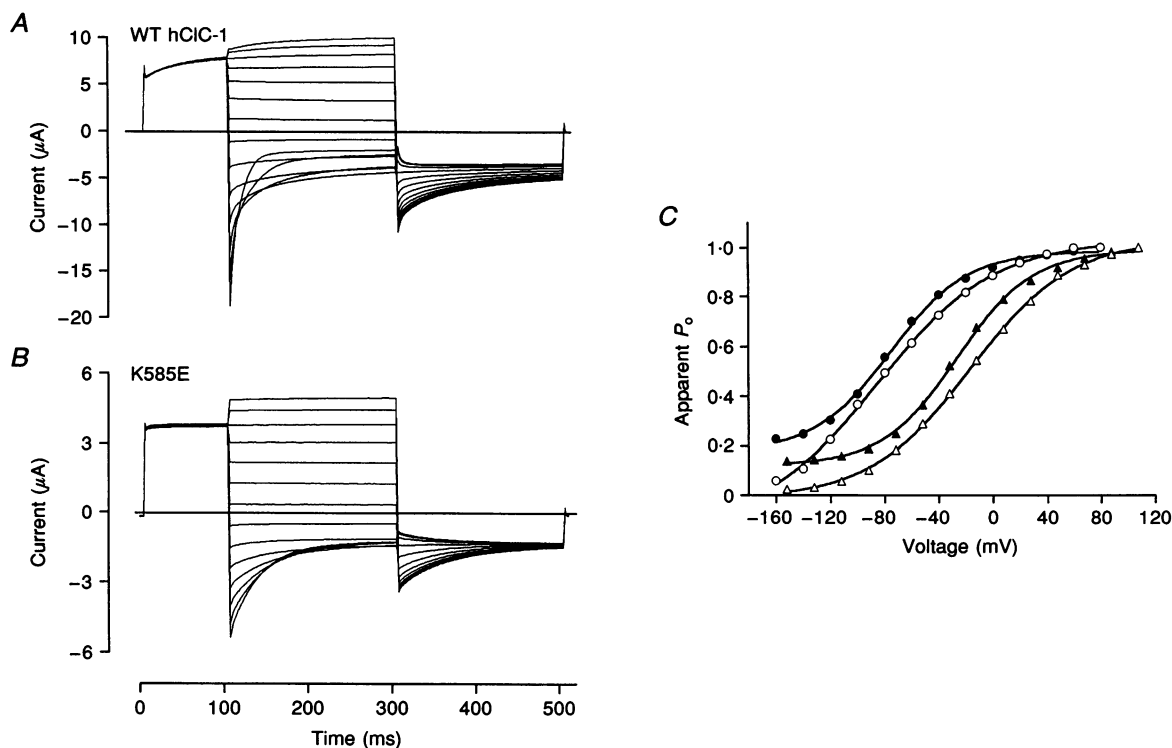


Figure 3. Voltage- and Cl⁻-dependent gating of hClC-1 expressed in *Xenopus* oocytes

A, current traces in an oocyte expressing WT hClC-1 were elicited by voltage-clamp test pulses at 20 mV increments between -160 and $+100$ mV. First, currents were strongly activated by a prepulse to $+60$ mV; then the voltage was stepped to the various test potentials. Apparent P_o , as plotted in C, was again determined from the tail currents. B, current traces, recorded as in A, from the mutant K585E. C, apparent P_o of WT hClC-1 determined in ND96 (103.6 mM [Cl⁻]_o; ○) and in 23.6 mM [Cl⁻]_o (△). Continuous lines represent fits of a Boltzmann distribution (including a constant offset, X_o). Measurements from several oocytes yielded a half-maximal voltage, $V_{1/2}$, of -62 ± 6 mV ($n = 10$, means \pm s.d.), an apparent gating charge, z , of 0.89 ± 0.05 , and an offset, X_o , of 0.01 ± 0.01 . In 23.6 mM [Cl⁻]_o these values were: $V_{1/2} = -2 \pm 6$ mV ($n = 10$); $z = 0.85 \pm 0.04$; and $X_o = 0.01 \pm 0.01$. For the K585E mutant, apparent P_o was again determined in ND96 (103.6 mM [Cl⁻]_o; ●) and in 23.6 mM [Cl⁻]_o (▲). Note the significant offset of P_o at negative voltages. Gating parameters for mutant K585E are: $V_{1/2} = -59 \pm 7$ mV ($n = 4$); $z = 0.89 \pm 0.06$; and $X_o = 0.26 \pm 0.01$ in ND96; and $V_{1/2} = -16 \pm 6$ mV; $z = 0.96 \pm 0.04$; and $X_o = 0.18 \pm 0.02$ in low [Cl⁻]_o.

glutamate because this had the same effect as replacing external NaCl with glucose. We had found that some impermeant anions were not innocuous as Cl^- substitutes, blocking or otherwise interfering with channel gating processes. For example, when methanesulphonate replaced 95% of external Cl^- , up to two-thirds of peak current was blocked at -120 mV and the apparent P_o curve was shifted in the hyperpolarizing direction by about 50 mV ($V_{1/2}$, -135 ± 2 mV).

To test whether the effects of Cl^- reduction should be attributed to external Cl^- alone or to the change in driving force for Cl^- , outward currents were monitored while internal Cl^- was steadily decreased. This was achieved over several minutes, immediately after formation of a whole-cell patch using a pipette containing zero Cl^- (glutamate as substitute). During this period, outward currents were constant despite a diminishing internal Cl^- concentration as the cellular contents equilibrated with the patch pipette. In other experiments, after cellular contents had equilibrated with pipette Cl^- concentrations ranging from 5 to 170 mM, apparent P_o curves were not shifted on the voltage axis, in contrast to the effect of external Cl^- .

The K585E mutant of ClC-1 resembles the equivalent ClC-0 mutant

Dependence of gating parameters on voltage and external Cl^- in hClC-1, as measured in *Xenopus* oocytes, is very similar to that of rClC-1. Deactivation of currents at hyperpolarizing potentials (Fig. 3A) can again be described by the sum of two exponential components and a voltage-dependent steady-state component (Table 1), with apparent P_o shifted to more depolarizing potentials by low external $[\text{Cl}^-]$ (Fig. 3C). Differences include a slightly flatter apparent P_o curve for hClC-1 compared with rClC-1, and the peak of the suggested, weakly parabolic relationship between τ_1 and voltage (if this is real) is shifted by around +50 mV at a given external Cl^- concentration (Table 1), which could explain the seemingly opposite voltage dependencies of τ_1 in the measurable range at normal external $[\text{Cl}^-]$.

We have investigated the similarity between gating in ClC-1 and ClC-0 by producing the K585E mutant, equivalent to the K519E mutation of ClC-0 studied by Pusch *et al.* (1995a). Figure 3B shows clearly that gating is much slower in K585E than in WT hClC-1 and, interestingly, a single exponential (probably τ_2) is now sufficient to describe

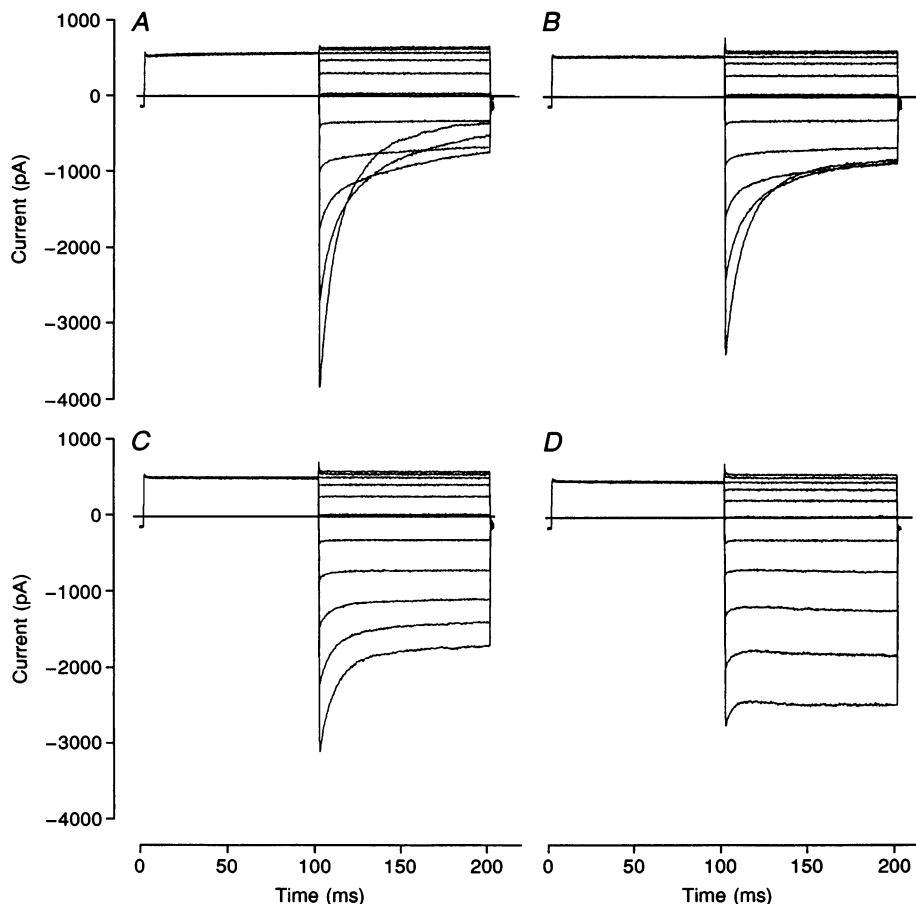


Figure 4. The dependence of rClC-1 gating on the external pH

Using the voltage protocol described in Fig. 1, Cl^- currents were recorded at pH_o 7.5 (A), pH_o 6.5 (B), pH_o 6.0 (C) and pH_o 5.5 (D). Internal pH in all experiments was 7.2.

deactivation. Its time constant is at least 2-fold larger than the slow time constant of WT hClC-1 at -140 and -120 mV (Table 1). Unfortunately, differences in kinetics are difficult to compare at less hyperpolarizing voltages because the very slow component (τ_2) in WT hClC-1 becomes progressively more prominent. Also, this component is greatly diminished in the mutant K585E. This difference is obvious from comparison of tail currents (Fig. 3A and B); there is rapid convergence to the steady state in the mutant but not in WT hClC-1. Open probability is still Cl⁻ dependent (Fig. 3C), similar to WT ClC-1. As with ClC-0, the K585E mutation induces incomplete closure of the fast gate at hyperpolarizing potentials, indicated by the small but significant offset of ~18% in the apparent P_o (Fig. 3C). Open pore properties are again significantly changed: the instantaneous $I-V$ relationship of the mutant in 104 mM Cl⁻ is almost linear, in contrast to the inwardly rectifying $I-V$ relationship of WT hClC-1.

Low pH_o enhances steady-state current at the expense of deactivating components

Both inward and outward currents are profoundly affected by reducing external pH (Fig. 4), peak currents being reduced by about 20–30% at pH_o 5.5, with deactivation decreasing and steady-state inward currents correspondingly increasing. These effects appear to be titrated with a pK_a of approximately 6. By contrast with the effects of decreasing external [Cl⁻], a reduction in external pH does not obviously alter either the fast or the slow time constants of deactivation (Table 1), although these are increasingly difficult to extract from the records as the amplitudes of the deactivating portions of the currents become smaller. There

are substantial effects on the relative proportions of the current components (Fig. 5), steady-state current being greatly increased with a concomitant reduction in both exponentially decaying components. Curves indicating relative proportions of the different current components, with respect to voltage, are illustrated. Data points for the fast and steady-state components are fitted by Boltzmann distributions B_1 and B_2 with the data points for the slow component being fitted by $1 - (B_1 + B_2)$ in each case. Despite the dramatic changes as pH_o is reduced, the three components of the inward current retain their voltage dependence (Fig. 5), and P_o curves are shifted only slightly on the voltage axis (Fig. 2). Plainly, the Boltzmann curves fitted to the data in Fig. 2 for pH_o ≤ 6.5 are much less steep than the curve for pH_o 7.5, but this is mainly due to an increasing offset (X_o) and neither $V_{1/2}$ nor the slope factor, k , are appreciably influenced by pH_o (Table 2). The offset takes into account that proportion of the current which acts as though it were flowing through permanently open channels, while the actual Boltzmann relationship applies only to the decaying portion of the current and this is greatly reduced as pH_o decreases. By pH_o 5.5, the decaying currents have become too small for accurate extraction of data. All these effects of low external pH are fully reversible on return to control solution.

At low external pH, ClC-1 kinetics are independent of external Cl⁻ concentration

Current kinetics are strongly dependent on external Cl⁻ concentration at normal external pH (Fig. 1). As external pH is reduced, the deactivating components of the inward current decrease and eventually practically disappear

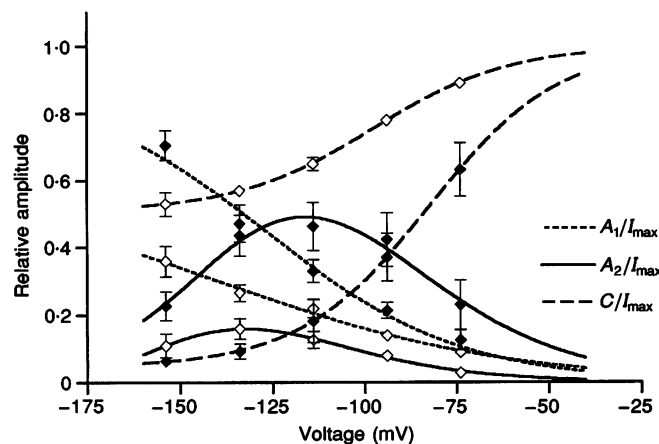


Figure 5. Effect of external pH on the voltage dependence of the components of the rClC-1 current

The contribution of each component is plotted as a fraction of the total current. Whole-cell currents were fitted by a non-linear least-squares method to an equation of the form $I(t) = A_1 \exp(-t/\tau_1) + A_2 \exp(-t/\tau_2) + C$, where A_1 and A_2 represent the amplitude of the fast and slow exponential components, respectively, C represents the amplitude of the steady-state component and t is time. I_{\max} is current at time zero. Results are plotted as the means \pm s.d. ($n = 12$ for pH_o 7.5 (◆) and $n = 4$ for pH_o 6.0 (◇)). Liquid junction potentials have been corrected.

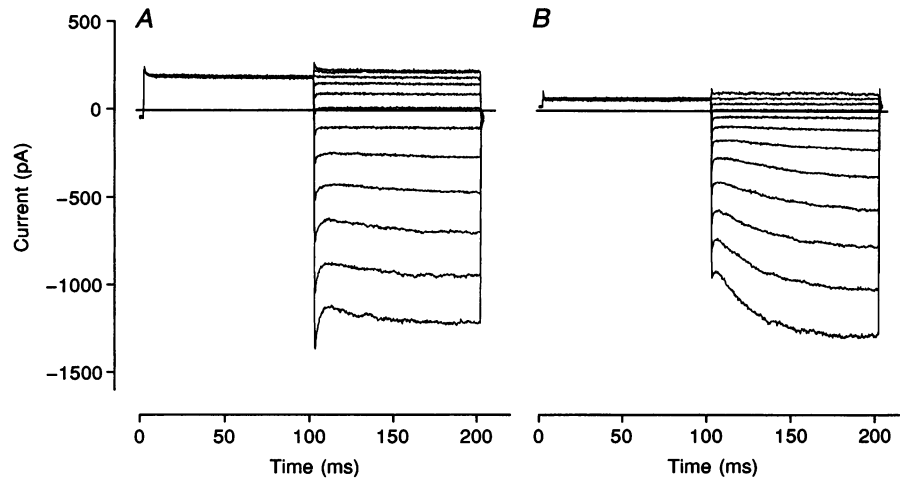


Figure 6. Effect of $[\text{Cl}^-]_o$ on gating of rClC-1 at low external pH

Cl^- currents were recorded at an external pH of 5.5 when cells were stepped to potentials ranging from -140 to $+80$ mV for 100 ms following a prepulse to $+40$ for 100 ms from holding potentials of -30 mV (A) or $+30$ mV (B) with an external $[\text{Cl}^-]$ of 174 mM (A) or 8 mM (B).

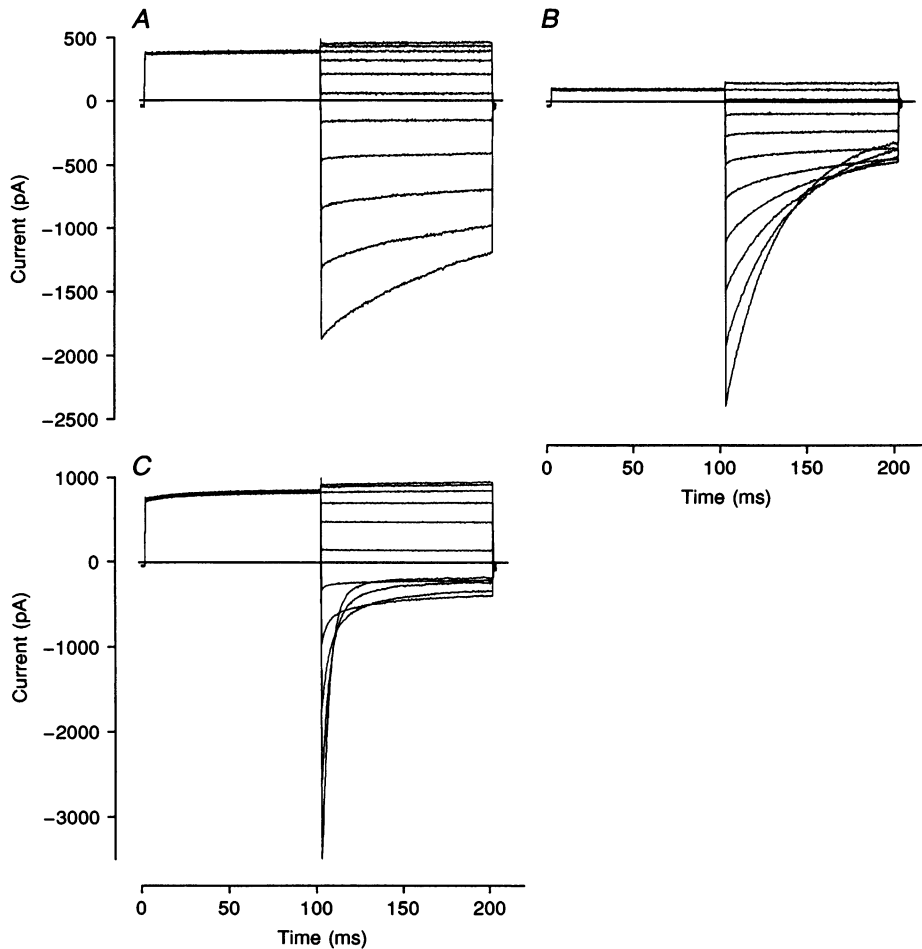


Figure 7. Effect of low $[\text{Cl}^-]_o$ and of internal benzoate on the kinetics of the rClC-1 current at low internal pH

Chloride currents were recorded at an external $[\text{Cl}^-]$ of 174 mM (A) or 8 mM (B). In C, external $[\text{Cl}^-]$ was 174 mM and 20 mM of the internal glutamate was replaced by benzoate. Internal $[\text{Cl}^-]$ was 40 mM and internal pH was 5.6 throughout. Voltage protocol was the same as that used in Fig. 1 with holding potentials of -30 mV (A and C) or $+30$ mV (B).

(Fig. 4), suggesting that there has been an overwhelming change in the gating process. We therefore again tested the effects of modifying external Cl⁻ concentration. At pH_o 5.5, the exponentially decaying components are not enhanced by low external [Cl⁻] and the remaining steady-state currents are independent of external [Cl⁻] (Fig. 6 and cf. Fig. 1). The increasing current activation at hyperpolarizing potentials (Fig. 6B) results from the more depolarized holding potential (as explained later in relation to Fig. 9).

Deactivation kinetics are strongly dependent on internal pH

Alteration of internal pH has very different effects. When a whole-cell patch is obtained using an electrode filled with a solution at a pH_i lower than 7, the deactivation kinetics are gradually slowed to reach a new stable condition after 5–10 min (cf. Figs 1A and 7A and Table 1). But if external Cl⁻ is now reduced, the rate of deactivation is increased (Fig. 7B and Table 1), just as occurs at normal internal pH (Fig. 1B). This is in contrast to the lack of effect of external Cl⁻ on deactivation kinetics when external pH has been reduced (Fig. 6). At the same time as low internal pH slows kinetics, the P_o curve is shifted in the hyperpolarizing direction (Fig. 8). It then becomes difficult to sustain the very negative potentials necessary to determine whether the apparent P_o decreases towards zero, as at normal pH, or whether there is a remaining offset, as at low external pH. Reducing external [Cl⁻], however, shifts the P_o curve to the right, exactly in parallel, and under these conditions there is essentially no remaining offset (Fig. 8). Therefore, in contrast to the situation at low external pH (Fig. 2), the data obtained at low internal pH can be fitted by Boltzmann distributions with zero or a very small offset (X_o) and, at constant external Cl⁻ concentration, display a conspicuous

hyperpolarizing shift in V_{1/2} along with a decreased slope (Fig. 8). Raising internal pH to 8 speeds up deactivation (Table 1) and shifts the P_o curve in the depolarizing direction (Fig. 8). Details of V_{1/2} and slope factor, *k*, are compiled in Table 2. Just as when external pH is modified, the effects of modifying internal pH are fully reversible. This was shown by the sequential achievement of whole-cell patches on the same cell with, for example, high followed by low and then high pH in the patch pipette.

Internal benzoate mimics the effect of increasing internal pH

The slowed deactivation kinetics seen when pH_i is reduced can be reversed by addition of benzoate to the internal solution. Replacing 20 mM of the internal glutamate with benzoate at a pH_i of 5.6 (19.2 mM of free benzoate, since benzoic acid has a pK_a of 4.2) results in deactivation kinetics as fast as those otherwise occurring at an internal pH of 8 (Fig. 7C).

Slow gates are revealed at an external pH of 5.5

Inward currents at an external pH of 5.5 show some slow activation (Fig. 4D) which increases in prominence at more positive holding potentials (Fig. 6B). In whole-cell patches formed at an internal pH of 6.2, subsequent reduction of external pH to 5.5 reduces outward current by between 30 and 50% but instantaneous and steady-state currents are little different from each other (Fig. 9A). Holding at +40 mV for periods as long as 10 s between test pulses (Fig. 9B), however, greatly reduces outward and instantaneous currents and reveals a large hyperpolarization-activated current. Deactivation of these slow gates is considerably faster and more complete at low than at high pH_i, opposite to deactivation of the fast gates.

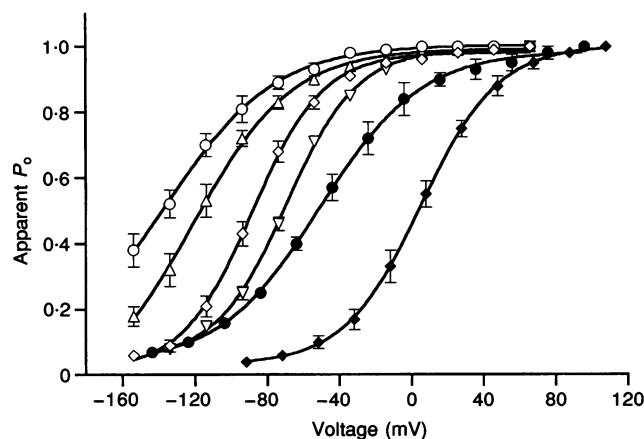


Figure 8. Apparent P_o of rClC-1 as a function of membrane potential at different values of internal pH and [Cl⁻]_o

Apparent P_o was determined as in Fig. 2. The external pH for all experiments was 7.5. Results are shown as means ± s.d. Values for internal pH and external [Cl⁻]_o were: pH_i 5.6, 174 mM [Cl⁻]_o (○); pH_i 6.2, 174 mM [Cl⁻]_o (△); pH_i 7.2, 174 mM [Cl⁻]_o (◇); pH_i 8.0, 174 mM [Cl⁻]_o (▽); pH_i 5.6, 8 mM [Cl⁻]_o (●); and pH_i 7.2, 8 mM [Cl⁻]_o (◆). Numbers in each experimental category are as listed in Table 2. The continuous lines represent fits of a Boltzmann distribution. Liquid junction potentials have been corrected.

DISCUSSION

A voltage sensor intrinsic to the protein is not essential for voltage-dependent gating

In the absence of single channel studies, which, anyway, are unlikely to be feasible for a single channel conductance of 1 pS (Pusch *et al.* 1994), a number of mechanisms could be proposed to account for the deactivating currents of ClC-1 with two, or even three, exponential components. Such deactivation might be explained by any of several complex forms of voltage-dependent gating relaxation, such as switching from bursting to non-bursting modes or switching from a preponderance of higher to one of lower conductance substates. There are also other possibilities, for example, voltage-dependent gating plus voltage-dependent block, or gating that is independent of voltage while current flow is impeded by more than one form of voltage-dependent block. Work on ClC-0 suggests that, although membrane potential modulates P_o , this is unlikely to be via an intrinsic voltage sensor, such as the S4 segment of voltage-gated cation channels, but rather reflects an indirect influence of voltage via Cl^- concentration dependence (Pusch *et al.* 1995a). A similar mechanism might operate in ClC-1, although this view is not shared by Fahlke *et al.* (1995, 1996), who have proposed a conventional model of gating dependent on voltage sensors.

Gating depends on external Cl^- concentration and not on the Cl^- gradient

We presume that the reduction and virtual disappearance of inward Cl^- currents when external Cl^- is reduced is due to a decrease in the open probability of ClC-1 channels since it is difficult to conceive of a mechanism that would reduce single channel inward current (equivalent to outflow of Cl^-) while internal Cl^- concentration is maintained constant. If, under conditions of low external Cl^- , the holding potential is

shifted closer to the Cl^- equilibrium potential, then inward currents are restored, showing that dependence on external Cl^- is itself voltage dependent, in the steady state. There is no dependence, however, on internal Cl^- , since the amplitude of outward currents is unaffected by altering internal $[\text{Cl}^-]$. Although obviously depending on external $[\text{Cl}^-]$, P_o cannot, then, be linked to the transmembrane Cl^- gradient. This behaviour is, in some ways, analogous to that of certain K^+ inward rectifier channels which are similarly dependent on the external but independent of the internal K^+ concentration (Hagiwara & Yoshii, 1979). Our observations refute the model of Fahlke *et al.* (1996) and support that of Pusch *et al.* (1995a).

An internal Cl^- -binding site accessible only to the exterior is implicated

Implicit in our findings is the suggestion that permeation through the ClC-1 channel is controlled by a binding site for Cl^- which is accessible only from the external solution and which must be occupied for opening to occur (at normal external pH). It must, furthermore, be situated inside the channel protein, where it is exposed to a local Cl^- concentration that depends on: (a) accessibility from the external bulk solution; (b) the concentration of Cl^- in the external solution; and (c) accumulation or depletion due to the imposed transmembrane potential. If the binding site is inside the conducting pore of the channel protein, then our findings are also consistent with the presence of a gate at the cytoplasmic end of the pore, as has been postulated for ClC-0 (Pusch *et al.* 1995a). One component of the current decay at hyperpolarizing potentials could then be related to a decreasing Cl^- concentration near the binding site, a consequent shift in the binding equilibrium toward dissociation and an accompanying decrease in P_o .

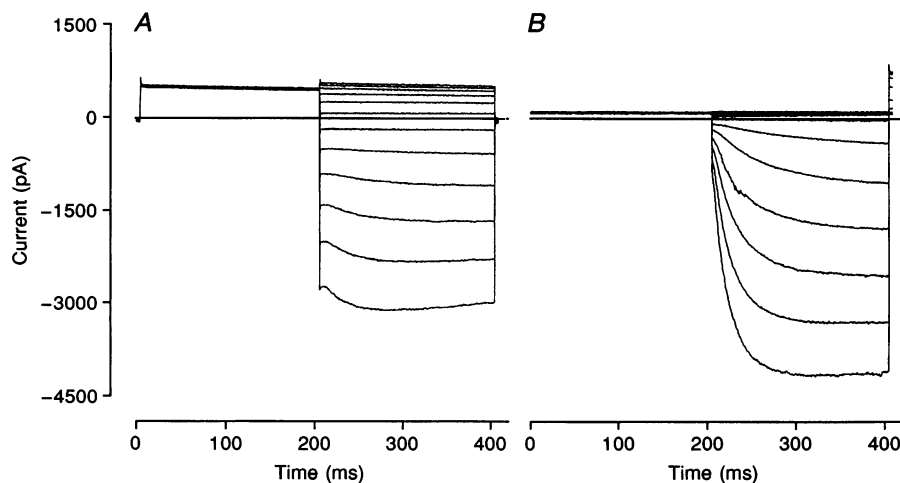


Figure 9. Activation of the slow gate of rClC-1 at low external pH

Again using the same voltage protocol as in Fig. 6, Cl^- currents were recorded at an external $[\text{Cl}^-]$ of 174 mM and an internal pH of 6.2. The effects of reducing external pH to 5.5 are shown for holding potentials of -30 mV in A and $+40$ mV in B. The interval between pulses was 10 s.

Gating in ClC-1 resembles fast gating in ClC-0 and is similarly modified by K585E

Results obtained with rClC-1 in Sf-9 cells and with WT and mutant K585E hClC-1 in *Xenopus* oocytes show that fast gating in ClC-1 must have a very similar underlying mechanism to that of ClC-0 and they support the contention that gating is dependent on the permeating anion. Large external anions such as glutamate must then be unable to gain access to the binding site that controls gating. Just as in ClC-0, the gating charge in ClC-1, as reflected in the Boltzmann slope factor (Table 2), is approximately one. That the gating relaxations for K585E can be fitted by single exponential functions, compared with at least a double exponential time course for WT ClC-1, is not easy to understand. Most probably, the relative contribution of the fast, weakly voltage-dependent component, is diminished in the mutant in favour of the slow, more voltage-dependent component. Where both exponentials can be followed in WT ClC-1 it is apparent that the slow component is smaller and faster at low Cl⁻ concentration and at more negative potentials. It may be this component of the current that is dependent on the rate of Cl⁻ dissociation from the putative gating control site, but with a time constant in the range of 10–80 ms, the apparent reaction rate would be too slow to reflect individual ion permeation through the channel pore. Also, because apparent P_o is dependent only on external Cl⁻ concentration, Cl⁻ ions traversing the channel as the Cl⁻ current must not be individually required to bind to the control site. Other possible mechanisms might also contribute to current deactivation at hyperpolarizing potentials, for example, the rate of dissociation of Cl⁻ from its binding site could depend directly on a potential-dependent protein conformation change or, at negative potentials, entry of internal blocking anions into the cytoplasmic end of the channel could be enhanced. In any case, with several exponential components in its gating relaxations, the gating mechanism for ClC-1 must be considerably more complicated than that of ClC-0. Further structure–function studies are needed to resolve these differences. Instantaneous (open channel) I – V relationships are also distinctly different in ClC-0 and ClC-1. Whereas ClC-1 shows strong inward rectification at positive voltages, ClC-0 has a linear I – V relationship. The effect of the mutant K585E on rectification, however, parallels the effect of the equivalent mutation in ClC-0, where channels become outwardly rectifying. In ClC-1, the instantaneous I – V relationship for the mutant K585E is converted from inwardly rectifying to linear, i.e. a change towards outwardly rectifying, compared with WT ClC-1.

Some poorly permeant anions may be able to replace Cl⁻ in the control of gating

Fahlke *et al.* (1995, 1996) have proposed that ClC-1 has evolved a gating mechanism which is distinct from that of ClC-0 and which uses voltage sensors. In support of their proposal, they have reported a shift of the apparent P_o

curve for WT hClC-1 in the hyperpolarizing direction when external Cl⁻ concentration is reduced by methanesulphonate replacement. The reported voltage shift, which we have confirmed, is opposite to that which has been described for ClC-0 (Pusch *et al.* 1995a) and which we have found for both rClC-1 and hClC-1 when Cl⁻ is replaced by glutamate or glucose. In our experience, some organic anions, such as methanesulphonate, seem able to replace Cl⁻ as the channel opener although they are themselves poorly permeant (authors' unpublished observations). The result of partial replacement of external Cl⁻ by such an anion might then be no shift of the P_o curve or a shift in the hyperpolarizing direction and must not be interpreted as implying that the gating of ClC-1 is independent of Cl⁻ or that it differs fundamentally from the Cl⁻-dependent gating of ClC-0.

Dependence on internal pH suggests block or allosteric modification by hydroxyl ions

Raised intracellular pH changes kinetics and P_o in a manner resembling a reduction of extracellular [Cl⁻], shifting the voltage dependence of gating towards positive potentials. Such a shift may indicate a change in the relative free energies of open and closed states upon titration of intracellular side-chains of the channel protein. This is analogous to the situation with ClC-1 mutants identified in dominant human myotonia, where several mutations at very different positions result in a drastic shift of voltage dependence in the same direction (Pusch *et al.* 1995b). A relatively flat titration curve, as found in our experiments, could imply that a number of different sites with different pK values are involved. The effect of intracellular benzoate is more difficult to explain because it seems unlikely that benzoate could compete with OH⁻ ions for titratable sites. This argues against the 'ball and chain' cytoplasmic gate of Fahlke *et al.* (1996). Moreover, it is not apparent why the Boltzmann slope factor, and hence the nominal gating charge, should be changed by pH_i. As an alternative to the allosteric modulation of a Cl⁻-dependent gating process by pH_i and benzoate, one could consider a blocking effect of OH⁻ ions or benzoate, possibly directly at the pore. However, if fast deactivation at hyperpolarization is caused directly by a voltage-dependent block due to intracellular OH⁻ ions, it is unclear how the interaction with extracellular anions occurs. One might imagine that blocking of the pore by OH⁻ ions somehow interferes with (extracellular) Cl⁻-binding to its site in the pore, but clearly more work is needed to distinguish between this model and the allosteric effect described above. Interestingly, the mutated site in K585E is putatively placed at the inner end of the channel pore, converting a highly conserved positively charged residue to one that is negatively charged. This might interfere with the ability of OH⁻ ions to enter the pore from the internal solution to block the channel directly or to influence the Cl⁻-binding site. Absence of a fast component of deactivation in the mutant might thus be explained. Overall, the effects of internal pH on ClC-1 are consistent with those observed in

CIC-0 reconstituted into lipid bilayers (Hanke & Miller, 1983), where decreasing pH shifts the P_o curves to more hyperpolarizing potentials and concomitant changes in single channel kinetics would be expected to slow macroscopic current deactivation.

In CIC-1 the Cl⁻-binding site that controls gating can be influenced by protonation

When external pH is lowered, its effect totally overrides kinetic modifications induced by previous manipulation of internal pH. Change of the external pH, no matter what the internal pH is, changes the relative proportions of steady-state and instantaneous current without significantly altering the kinetics of the remaining deactivating portion of the current. The components remain dependent on potential at low pH_o (Fig. 6), without substantial shift on the voltage axis. While our results at normal and low pH_o are well fitted by Boltzmann distributions B_1 and B_2 , the physical interpretation of this remains unclear. With reduction of external pH, it is likely that a single site, accessible only from the outside, is protonated since the titration curve appears to be steep around a pK of about 6. Protonated channels lose their ability to deactivate at negative potentials, possibly as a result of increased affinity of the binding site for Cl⁻, perhaps with the rate of dissociation of Cl⁻ from the site no longer depending on potential. With respect to the apparent reduction in the postulated block by internal hydroxyl ions at low external pH, strong binding of Cl⁻ might prevent hydroxyl from blocking the channel so effectively. An increase in binding constant could be mediated by direct protonation of the Cl⁻-binding site or by a conformational change caused by protonation in some other part of the channel protein, but it is clear that, wherever it is, the site of protonation must be accessible only from the external solution, just as the Cl⁻-binding site is for Cl⁻ ions. Our results are entirely consistent with those of Warner (1972) using the three-electrode voltage-clamp on whole frog muscle. What is uncertain, however, also from Warner's results, is exactly how an enhanced steady-state component can be compatible with the reduced membrane conductance determined in whole muscle at low pH by cable analysis (Hutter & Warner, 1967; Palade & Barchi, 1977). The profound influence of external pH on CIC-1 is in strong contrast to its apparent lack of effect on CIC-0 (Hanke & Miller, 1983), where the effect of pH manipulation could be entirely accounted for by action from the *cis* side (equivalent to the inside, cf. Bauer *et al.* 1991).

Aspartate 136 may provide a clue about the control of slow gating

In CIC-1, low external pH exposes a hyperpolarization-activated slow gate which has characteristics somewhat resembling the slow gates of CIC-0 and CIC-2. A similar pattern emerges in the hCIC-1 mutant, D136G, where outward currents are completely absent and deactivating inward currents are replaced by slowly activating currents at hyperpolarizing potentials (Fahlke *et al.* 1995). It is

possible that the similarity results from an equivalent change in charge (negative to neutral in the mutant or additional positive charge with protonation) at residue 136 or at a residue in close proximity to it. In WT CIC-1 at normal pH_o and normal holding potentials the slow gate must be continuously open. Its nature, its relationship to the slow gate of CIC-0 and whether or not it has Cl⁻ dependence remain to be determined. In view of the interaction of methanesulphonate with the channel (discussed above), the conclusions of Fahlke *et al.* (1995, 1996), with respect to the Cl⁻ dependence of D136G, are not convincing.

- ASTILL, D. ST J., RYCHKOV, G. Y., CLARKE, J. D., HUGHES, B. P., ROBERTS, M. L. & BRETAG, A. H. (1996). Characteristics of skeletal muscle chloride channel CIC-1 and point mutant R304E expressed in Sf-9 insect cells. *Biochimica et Biophysica Acta* **1280**, 178–186.
- BARRY, P. H. (1994). JPCalc, a software package for calculating liquid junction potential corrections in patch-clamp, intracellular, epithelial and bilayer measurements and for correcting junction potential measurements. *Journal of Neuroscience Methods* **51**, 107–116.
- BAUER, C. K., STEINMEYER, K., SCHWARZ, J. R. & JENTSCH, T. J. (1991). Completely functional double-barreled chloride channel expressed from a single *Torpedo* cDNA. *Proceedings of the National Academy of Sciences of the USA* **88**, 11052–11056.
- BIRNIR, B., TIERNEY, M. L., HOWITT, S. M., COX, G. B. & GAGE, P. W. (1992). A combination of human α_1 and β_1 subunits is required for formation of detectable GABA-activated chloride channels in Sf-9 cells. *Proceedings of the Royal Society B* **250**, 307–312.
- BRETAG, A. H. (1987). Muscle chloride channels. *Physiological Reviews* **67**, 618–724.
- FAHLKE, C., ROSENBOHM, A., MITROVIC, N., GEORGE, A. L. & RÜDEL, R. (1996). Mechanism of voltage-dependent gating in skeletal muscle chloride channels. *Biophysical Journal* **71**, 695–706.
- FAHLKE, C. & RÜDEL, R. (1995). Chloride currents across the membrane of mammalian skeletal muscle fibres. *Journal of Physiology* **484**, 355–368.
- FAHLKE, C., RÜDEL, R., MITROVIC, N., ZHOU, M. & GEORGE, A. L. (1995). An aspartic acid residue important for voltage-dependent gating of human muscle chloride channels. *Neuron* **15**, 463–472.
- GEORGE, A. L., CRACKOWER, M. A., ABDALLA, J. A., HUDSON, A. J. & EBERS, G. C. (1993). Molecular basis of Thomsen's disease (autosomal dominant myotonia congenita). *Nature Genetics* **3**, 305–310.
- GRONEMEIER, M., CONDIE, A., PROSSER, J., STEINMEYER, K., JENTSCH, T. J. & JOCKUSCH, H. (1994). Nonsense and missense mutations in the muscular chloride channel gene *clc-1* of myotonic mice. *Journal of Biological Chemistry* **269**, 5963–5967.
- GRÜNDER, S., THIEMANN, A., PUSCH, M. & JENTSCH, T. J. (1992). Regions involved in the opening of CIC-2 chloride channel by voltage and cell volume. *Nature* **360**, 759–762.
- HAGIWARA, S. & YOSHII, M. (1979). Effects of internal potassium and sodium on the anomalous rectification of the starfish egg as examined by internal perfusion. *Journal of Physiology* **292**, 251–265.
- HANKE, W. & MILLER, C. (1983). Single chloride channels from *Torpedo* electroplax: Activation by protons. *Journal of General Physiology* **82**, 25–45.

- HUTTER, O. F. & WARNER, A. E. (1967). The pH sensitivity of the chloride conductance of frog skeletal muscle. *Journal of Physiology* **189**, 403–425.
- KOCH, M. C., STEINMEYER, K., LORENZ, C., RICKER, K., WOLF, F., OTTO, M., ZOLL, B., LEHMANN-HORN, F., GRZESCHIK, K.-H. & JENTSCH, T. J. (1992). The skeletal muscle chloride channel in dominant and recessive human myotonia. *Science* **257**, 797–800.
- MIDDLETON, R. E., PHEASANT, D. J. & MILLER, C. (1994). Purification, reconstitution, and subunit composition of a voltage-gated chloride channel from *Torpedo* electroplax. *Biochemistry* **33**, 13189–13198.
- MILLER, C. (1982). Open-state substructure of single chloride channels from *Torpedo* electroplax. *Philosophical Transactions of the Royal Society B* **299**, 401–411.
- PALADE, P. T. & BARCHI, R. L. (1977). Characteristics of the chloride conductance in muscle fibers of the rat diaphragm. *Journal of General Physiology* **69**, 325–342.
- PUSCH, M., LUDEWIG, U., REHFELD, A. & JENTSCH, T. J. (1995a). Gating of the voltage-dependent chloride channel ClC-0 by the permeant anion. *Nature* **373**, 527–531.
- PUSCH, M., STEINMEYER, K. & JENTSCH, T. J. (1994). Low single channel conductance of the major skeletal muscle chloride channel, ClC-1. *Biophysical Journal* **66**, 149–152.
- PUSCH, M., STEINMEYER, K., KOCH, M. C. & JENTSCH, T. J. (1995b). Mutations in dominant human myotonia congenita drastically alter the voltage-dependence of the ClC-1 chloride channel. *Neuron* **15**, 1455–1463.
- RICHARD, E. A. & MILLER, C. (1990). Steady-state coupling of ion-channel conformations to a transmembrane gradient. *Science* **247**, 1208–1210.
- STEINMEYER, K., KLOCKE, R., ORTLAND, C., GRONEMEIER, M., JOCKUSCH, H., GRÜNDER, S. & JENTSCH, T. J. (1991a). Inactivation of muscle chloride channel by transposon insertion in myotonic mice. *Nature* **354**, 304–308.
- STEINMEYER, K., LORENZ, C., PUSCH, M., KOCH, M. C. & JENTSCH, T. J. (1994). Multimeric structure of ClC-1 chloride channel revealed by mutations in dominant myotonia congenita (Thomsen). *EMBO Journal* **13**, 737–743.
- STEINMEYER, K., ORTLAND, C. & JENTSCH, T. J. (1991b). Primary structure and functional expression of a developmentally regulated skeletal muscle chloride channel. *Nature* **354**, 301–304.
- THIEMANN, A., GRÜNDER, S., PUSCH, M. & JENTSCH, T. J. (1992). A chloride channel widely expressed in epithelial and non-epithelial cells. *Nature* **356**, 57–60.
- WARNER, A. E. (1972). Kinetic properties of the chloride conductance of frog muscle. *Journal of Physiology* **227**, 291–312.

Acknowledgements

This study was supported by the Neuromuscular Research Foundation of the Muscular Dystrophy Association of South Australia, the Australian Research Council and the Research Committee of the University of South Australia (to A.H.B.) and by the Deutsche Forschungsgemeinschaft, Germany and the Muscular Dystrophy Association, USA (to T.J.J.). D.St.J.A. held a 'Ross Stuart Postgraduate Scholarship' of the Muscular Dystrophy Association of South Australia.

Author's email address

A. H. Bretag: a.bretag@unisa.edu.au